

Obliquely scattered echos from the north polar cap near Chasma Boreale showed the surface to be usually smooth during experiments performed with Viking Orbiter 2; if the icy surface is typically smoother than Mars plains on scales of centimeters to meters, the modeling needed for occultation corrections may be simpler than anticipated.

Backscattering experiments on icy planetary surfaces have yielded unusually high radar cross sections and unpredicted polarizations. The Galilean satellites of Jupiter, for example, return more energy toward Earth-based radar systems than is expected from polished metal spheres of the same dimensions. They also return signals with predominantly the same polarizations as transmitted, counter to expectations based on simple reflection mechanisms for smooth surfaces. The same behavior has been seen in radar echos from the residual south polar cap on Mars. Oblique scattering experiments in which the Mars Observer antenna is aimed toward icy surface targets rather than in its nominal Earth-point direction may allow measurements of the scattered signal under conditions that will allow estimation of scattering path lengths within the ice, an important parameter in determining the composition and history of the ice itself.

References: [1] Tyler G. L. et al. (1992) *JGR*, 97, 7759-7779. [2] Lindal G. F. et al. (1979) *JGR*, 84, 8443-8456.

WIND TRANSPORT NEAR THE POLES OF MARS: TIMESCALES OF CHANGES IN DEPOSITION AND EROSION. Peter C. Thomas, Center for Radiophysics and Space Research, Cornell University, Ithaca NY 14853, USA.

Movement of sediment into and out of polar deposits is intimately linked to the polar volatile budget and to changes in wind systems over the course of astronomically induced climate cycles. Our present observations of the morphology of polar layered deposits, mantling sediments, dune fields, and variable surface features are the basis of inferences on the efficacy of polar sediment transport mechanisms. The timescales of formation of these features vary from days to perhaps 10^6 yr, and latitudinal banding of dune fields near the poles may have been formed on timescales of 10^7 yr.

Orientations of intracrater dunes, dune crests, and wind streaks have been measured for latitudes -45 to -90 to compare features of likely different timescales of formation with models of wind flow from the south polar region. The larger features, such as intracrater dune fields, suggest formation primarily by winds flowing out from the pole with both prograde and retrograde components. The very long timescales of formation expected of the dune fields are consistent with their formation by strongest winds at different parts of the cycle of season of perihelion. The bedforms superposed on the dune fields, however, suggest winds somewhat less varied than those apparently recorded by the dune fields, and more

closely correlated with orientations of streaks from crater splotches and dune fields. This suggests that some bedforms of scales of about 100 m can be reoriented within one half of a cycle of season of perihelion (25,000 yr).

There is a complex variation with latitude of the indicated wind directions and of the efficacy of the resultant winds in orienting dune fields that suggests influence of frost cover on the ability of winds to move sediment in the spring and fall. Because of changes in the relative effectiveness of spring and fall winds expected with progression of the season of perihelion, the latitudinal variation in transport efficiency may mean that sediments at different latitudes dominantly respond to wind erosion and transport at different times during the perihelion cycle. The Viking data are too scattered in time to derive the controls on efficacy of fall and spring winds in detail, but monitoring by Mars Observer should allow generation of models of wind transport from and to the polar areas that may be extrapolated (with caution) to other parts of expected climate cycles. The likely long-term sedimentary balance of the polar deposits may then be more readily addressed.

N93-198209 f5
MODELING INTERANNUAL VARIABILITY IN THE MARTIAN SEASONAL CO₂ CYCLE. S. E. Wood and D. A. Paige, Department of Earth and Space Sciences, University of California, Los Angeles CA 90024, USA.

One of the most intriguing aspects of the seasonal pressure variations measured at the Viking Lander sites is their nearly perfect interannual repeatability [1,2]. This presents something of a problem, because it implies that the behavior of the seasonal polar caps should be highly repeatable from year to year as well. There are a number of observations and theories suggesting that the presence of dust and water ice clouds in the martian atmosphere should have significant direct and indirect effects on the rates of CO₂ condensation and sublimation in the north and south polar regions. These effects include (1) reduced rates of CO₂ frost condensation during polar night seasons due to the radiative effects of dust and water ice clouds [3-6] and associated CO₂ clouds [7,8] or elevated atmospheric temperatures [9,10] and (2) reduced or elevated rates of frost sublimation due to the radiative effects of atmospheric dust [6,11,12], or to changes in frost emissivities and albedos due to contamination by water ice and dust [8,13-15]. Because all these effects rely on the transportation of dust, water, and heat into the polar regions by the martian atmosphere, they are not expected to be exactly repeatable from year to year, especially given that two global dust storms were observed during the first Viking year, and none were observed the second and third [1,2,16]. Since all these effects could potentially contribute to the asymmetrical behavior of CO₂ frost at the north and south residual polar caps observed during the first Viking year

49069
 N93-19819 p.1

[12,17-19], assessing their impact on the present seasonal CO₂ cycle is of importance not only for understanding martian interannual climate variations, but long-term climate variations as well.

In this paper, we first examine the Viking Lander pressure observations themselves to determine the range and character of the interannual variations present. Then we use a diurnal and seasonal thermal model described by Wood and Paige [20] to quantitatively examine the effects of interannual variations in the polar heat balance on seasonal pressure variations.

Viking Lander Interannual Pressure Differences: Viking Landers 1 and 2 (VL1 and VL2) obtained surface pressure measurements during parts of four and two Mars years respectively [2]. We have examined the VL1 and VL2 daily averaged pressure data to determine the seasons and magnitudes of possible long-period interannual pressure variations [21]. At VL1, interannual pressure differences were typically less than 5 Pa from L_s 0 to L_s 180, but variability increased significantly between L_s 180 and L_s 360 [21]. During the 1977B global dust storm, average VL1 pressures were over 20 Pa higher than they were during the third year. The interannual pressure differences observed at VL2 show similar general trends to those observed at VL1, but the magnitudes are almost doubled [21]. Observed interannual pressure differences at VL2 were less than 5 Pa from L_s 120 to 180, but exceeded 20 Pa during the subsiding phases of the 1977A global dust storm, and exceeded 50 Pa during 1977B [21].

Overall, the results suggest that the interannual variability present in the Viking Lander pressure data may be due as much to interannual differences in atmospheric thermal and dynamic structure as to differences in atmospheric mass. An interannual variation in atmospheric mass would be expected to result in a pressure difference of the same sign at both landing sites. The large differences in average pressures that were observed during the 1977B global dust storm must also be partially due to atmospheric dynamic phenomena [22-24]. Despite potential ambiguities in their interpretation, the observed interannual pressure differences at the Viking Lander sites still place strong constraints on the potential magnitudes on interannual variations in the heat balance of the martian seasonal polar caps. In the following sections we take the observed VL1 interannual pressure differences as upper limits for interannual variations in the mass of the martian atmosphere.

Sensitivity to Year-Long Heat Balance Variations: Our experiences fitting the Viking pressure data [20] indicate that the martian seasonal pressure variations are extremely sensitive to year-long variations in the heat balance of the north and south seasonal polar caps. To demonstrate, we ran our diurnal and seasonal thermal model [20] for a number of years using a set of "standard best-fit" model input parameters that simultaneously fit the VL1 third-year seasonal pressure data and the retreat rates of the north and south seasonal

polar caps. Then we slightly altered the values of the best-fit albedos or emissivities of the seasonal frost deposits in either hemisphere through a complete cycle of polar cap growth and retreat. The results are presented in Table 1, which summarizes the standard best-fit model parameters, the alterations that were introduced, and the resulting maximum interannual pressure variations.

The results suggest that a uniform persistent interannual variation in the albedo or emissivity of the north or south seasonal polar cap of greater than 2% absolute would be quite apparent in the Viking Lander pressure data. Larger year-long interannual variations in the parameters could potentially be compatible with the available observations, but only if they occurred over limited periods of time and/or limited portions of the seasonal polar caps. Interannual pressure variations of these magnitudes would not be expected to produce large interannual variations in polar cap retreat rates.

TABLE 1. Year-long variations.

Parameter Changed	"Standard Best-fit" Value*	Perturbation Value	Max. Pressure Deviation	L _s of Peak
North Albedo	0.70	0.67	+10	50
North Emissivity	0.69	0.72	-11	12
South Albedo	0.54	0.51	+11	215
South Emissivity	0.71	0.68	+16	160

*Based on "standard best-fit" model using a total mass of CO₂ in the cap-atmosphere system of 210 kg/m², thermal inertia of soil in the northern hemisphere equal to 670 (MKS), and 167 (MKS) in the south.

Sensitivity to North Polar Warming: Both the Mariner 9 IRIS and Viking IRTM instruments observed significantly elevated atmospheric temperatures over the north seasonal polar cap during the 1971A and 1977B global dust storms [9,10]. For the case of the 1977B storm, IRTM 15-μm channel brightness temperatures exceeded 230 K at the edge of the polar night. Martin and Kieffer [10] have considered the downward flux of infrared radiation at the surface of the north seasonal polar cap due to these elevated atmospheric temperatures, and concluded that CO₂ condensation rates were substantially reduced for the cap as a whole during the peak of the storm. Near the edge of the cap, elevated atmospheric temperatures may have caused net CO₂ sublimation, amounting to perhaps as much as 13 Pa of CO₂ gas, globally averaged [10], which would be roughly consistent with the pressure increase observed at VL2.

Our thermal model [20] can be used to investigate some of the implications of the hypothesis that north polar cap CO₂ frost condensation was briefly halted during the 1977B storm. Figure 1 shows model-calculated surface pressures and north polar cap boundaries after a number of years of calculations

using the standard best-fit parameters, except during winter of the last year, when the emissivity of the entire north polar cap was decreased from 0.69 to 0.25 starting at L_s 280, and then increased back to 0.69 after 20 days. This effectively halts net frost condensation on the north seasonal cap as a whole during the period when elevated IRTM 15- μ m channel brightness temperatures were observed. Lowering the emissivity to zero would have resulted in net sublimation since the outer portions of the cap are outside the polar night.

As can be seen in Fig. 1, a brief cessation of frost condensation during the peak of the second global dust storm would have resulted in significantly elevated surface pressures at both landing sites that would not have disappeared until L_s 80 when the north seasonal polar cap had completely sublimated. If the north polar cap actually lost mass during the peak of the dust storm, the long-term effects on pressure would be greater still. This means that the true net effects of the elevated atmospheric temperatures on the heat balance of the north polar cap must have been smaller than estimated here, or these effects "healed" later in the winter due to increased frost condensation rates. Similar constraints must also apply to alternate mechanisms for reducing CO_2 frost condensation rates during the polar night that could exhibit interannual variability, such as the formation of atmospheric CO_2 clouds [7,8].

Sensitivity to North Polar Dust Contamination: Soon after the Viking discovery of the asymmetric behavior of seasonal frost at the north and south residual caps, it was pointed out that dust raised in the southern hemisphere during global dust storms could be transported northward and deposited onto the condensing north seasonal frost deposits, and lower the albedo of the polar cap during the following spring [25]. Pollack et al. [26] have estimated that as much as $0.02 \text{ g cm}^{-2} \text{ yr}^{-1}$ of dust was deposited north of $+60^\circ$ latitude during the first Viking year. Toon et al. [13] have calculated that only half this amount could lower pure frost albedos from 0.7 to 0.55. Warren et al. [14] have shown that depending on assumptions, the incorporation of dust into martian seasonal frost deposits could have even larger effects.

The potential effects of dust contamination on the behavior of the north seasonal polar cap can also be investigated using our thermal model [20]. The results presented in Table 1 show that a small year-long decrease in the albedo of either seasonal cap would have caused significant persistent interannual pressure variations. However, the results of these simulations may not be directly applicable to the situation where a layer of dark, dust-contaminated frost is deposited onto the condensing north seasonal polar cap during a global dust storm. Since such a dust layer would soon be covered by uncontaminated CO_2 frost, its effect on the polar cap's heat balance should not be apparent until most of the overlying uncontaminated CO_2 frost had sublimated. Figure 2 shows the results of a simulation where we ran the thermal model for a number of years using the standard best-fit model input

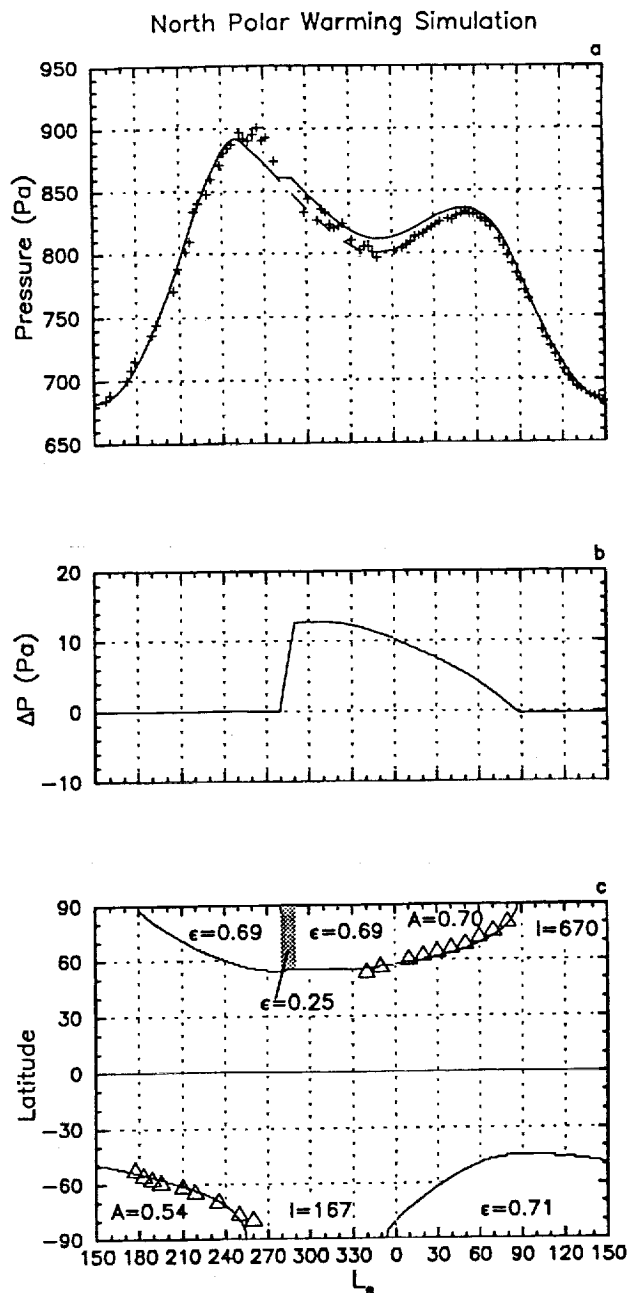


Fig. 1. (a) Model-calculated surface pressures (solid line) compared to VLI year 3 binned data (pluses). The "standard best-fit" parameters [A = frost albedo, ϵ = frost emissivity, I = soil thermal inertia (MKS)] were used until the last year when the north seasonal polar cap CO_2 frost emissivity was lowered to 0.25 from L_s 280 to 290.5 to simulate north polar warming during the 1977B global dust storm. Dashed line indicates unperturbed "standard best-fit" pressure curve. (b) Interannual variation in atmospheric pressure calculated by subtracting the best-fit pressure curve from the perturbed model-calculated pressures. The pressure difference increased at a constant slope until the emissivity was reset to 0.69. (c) Latitudinal extent of model-calculated seasonal polar caps and Viking Orbiter observations (triangles) of the retreating cap edges in 1977 [27,28] shown for comparison.

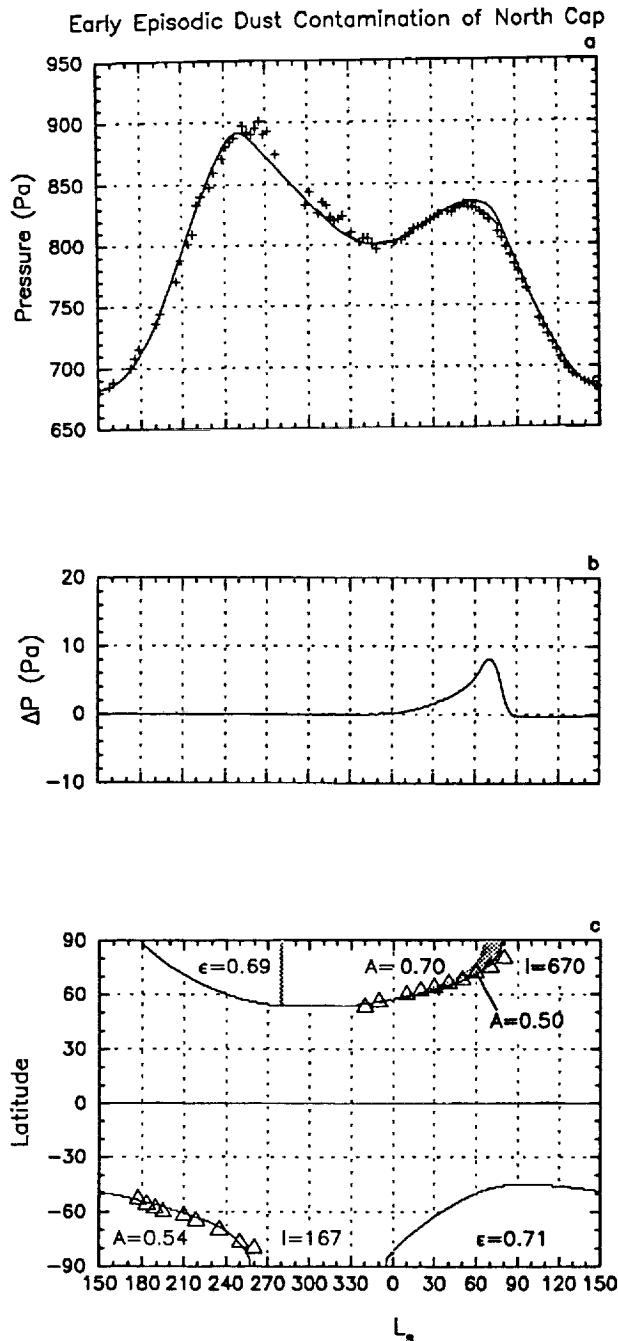


Fig. 2. Same format as Fig. 1. The "standard best-fit" parameters were used, but a "dust layer" was deposited onto the condensing north seasonal polar cap at L_s 280 with the initial phase of 1977B, then gradually exposed by sublimation of overlying CO_2 frost in the spring. This contaminated frost (indicated by shaded region after it is uncovered) was assumed to reduce the frost albedo from 0.70 to 0.50, resulting in higher sublimation rates. Although the observed pressure difference (b) is smaller than that resulting from the year-long 3% north polar cap albedo decrease indicated in Table 1, the effect on the retreat rate is slightly greater, causing the north seasonal cap (c) to disappear before L_s 80.

parameters, but during the winter of the final year, a dust layer was deposited onto the condensing north polar cap. The timing of the dust layer's deposition was assumed to coincide with the polar warming event associated with the initial phases of the 1977B dust storm at L_s 280. As the cap retreated during spring, the dust layer became exposed at the surface of the frost, first at the edge of the cap, and finally over the entire cap during the final stages of the retreat. Wherever the dust layer was exposed, seasonal frost albedos were assumed to decrease from their best-fit values of 0.7 to 0.5, and then were assumed to remain at 0.5 until the frost completely sublimated. The computed interannual pressure differences for this simulation increased sharply as the cap approached the final phase of retreat, but never exceeded 10 Pa. When compared to the first case listed in Table 1, the results presented in Fig. 2 are somewhat surprising, given the large changes in frost albedos that are assumed. We also performed other simulations for dust layers deposited later in the season, and found that the magnitudes of the computed pressure changes are larger because less frost forms over them and the dust is uncovered earlier.

Although these simulations are highly idealized, they demonstrate that the effects of episodic dust contamination events on the seasonal pressure curves may not be nearly as significant as expected. The signatures of these episodes on interannual pressure variations are peaked during the final retreat phases of the contaminated polar cap. Although incomplete, the VL1 data show no real indication of sustained elevated pressures during mid to late northern spring in any of the Viking years, and no evidence of the distinctive peak in interannual pressure differences during late spring. However, based on the amount of interannual variability present in the data, we estimate that these observations could potentially be compatible with the deposition of a dust layer at L_s 280 that had a spring season darkening effect of as much as 10% absolute. For a dust layer deposited at L_s 310, the darkening could be no more than 4% absolute. Since a difference between albedos of seasonal frost deposits at the north and south poles of this order could result in the observed asymmetry of the behavior of CO_2 frost at the north and south poles, the repeatability of the Viking seasonal pressure curves may not necessarily be incompatible with contamination of the accumulating north seasonal polar cap during global dust storms. Based on polar radiation balance measurements, Paige and Ingersoll [12] have estimated that the entire asymmetry can be explained by an approximately 20% absolute difference between the late spring albedos of the CO_2 frost deposits at the north and south residual polar caps. While it is not known whether this north-south difference is due entirely to differential dust contamination during global dust storms, the results of this study do not necessarily preclude this possibility.

References: [1] Leovy C. B. et al. (1985) *Recent Advances in Planetary Meteorology* (G. E. Hunt, ed.), 19-44, Cambridge, New York. [2] Tillman J. E. (1988) *JGR*, 93,

- 9433-9451. [3] Leovy C. B. (1966) *Science*, 154, 1178-1179.
- [4] Briggs G. A. (1974) *Icarus*, 23, 167-191. [5] James P. B. and North G. R. (1982) *JGR*, 87, 10271-10283. [6] Lindner B. L. (1990) *JGR*, 95, 1367-1379. [7] Paige D. A. (1985) Ph.D. dissertation, California Institute of Technology, Pasadena. [8] Pollack J. B. et al. (1990) *JGR*, 95, 1447-1473. [9] Hanel R. A. et al. (1972) *Science*, 175, 305-308. [10] Martin T. Z. and Kieffer H. H. (1979) *JGR*, 84, 2843-2852. [11] Davies D. W. (1979) *JGR*, 84, 8335-8340. [12] Paige D. A. and Ingersoll A. P. (1985) *Science*, 228, 1160-1168. [13] Toon O. B. et al. (1980) *Icarus*, 44, 552-607. [14] Warren S. G. et al. (1990) *JGR*, 95, 14717-14741. [15] James P. B. et al. (1990) *JGR*, 95, 1337-1341. [16] Colburn D. S. et al. (1988) *NASA TM-100057*. [17] Kieffer H. H. et al. (1976) *Science*, 194, 1341-1344. [18] Farmer C. B. et al. (1976) *Science*, 194, 1339-1341. [19] Kieffer H. H. (1979) *JGR*, 84, 8263-8288. [20] Wood S. E. and Paige D. A. (1992) *Icarus*, 99, 1-14. [21] Paige D. A. and Wood S. E. (1992) *Icarus*, 99, 15-27. [22] Haberle R. M. et al. (1982) *Icarus*, 50, 322-367. [23] Zurek R. W. (1982) *Icarus*, 50, 288-310. [24] Zurek R. W. and Haberle R. M. (1988) *J. Atmos. Sci.*, 45, 2469-2485. [25] Kieffer H. H. and Palluconi F. D. (1979) *2nd International Colloq. on Mars*, NASA CP-2072, 45-46. [26] Pollack J. B. et al. (1979) *JGR*, 84, 2929-2945. [27] James P. B. et al. (1979) *JGR*, 84, 2889-2922. [28] James P. B. (1979) *JGR*, 84, 8332-8334.